Biophysical Chemistry 254 (2019) 106240

Contents lists available at ScienceDirect

Biophysical Chemistry

journal homepage: www.elsevier.com/locate/biophyschem

Urea's match in the hydrogen-bond network? A high pressure THz study

Hendrik Vondracek[a], Serena Alfarano[a], Claudius Hoberg[a], Inga Kolling[a], Fabio Novelli[a], Federico Sebastiani[a], Jean-Blaise Brubach[b], Pascale Roy[b], Gerhard Schwaab[a], Martina Havenith[a,*]

[a] Ruhr-Universität Bochum, LS Physikalische Chemie II, Universitätsstraße 150, 44801 Bochum, Germany
[b] Ligne AILES - Synchrotron SOLEIL, L'Orme des Merisiers, F-91192 Gif-sur-Yvette, France

HIGHLIGHTS

- Solvation under extreme conditions
- High pressure studies
- Co-solvent effect of urea
- THz spectroscopy

GRAPHICAL ABSTRACT

The surrounding frame is 9 cm by 3.5 cm, which is the maximum permitted for Journal of the American Chemical Society graphical table of content entries.

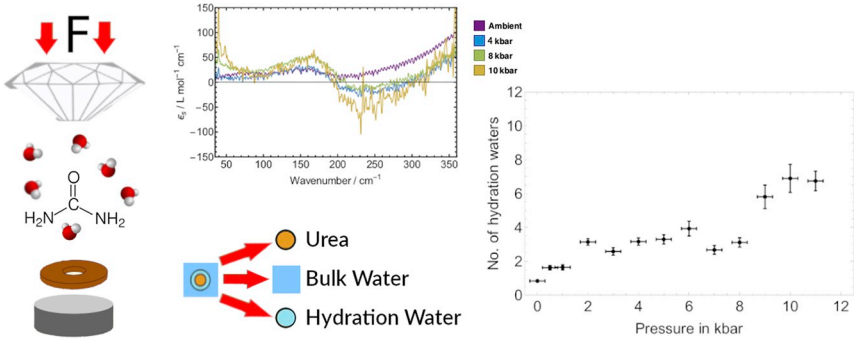

ABSTRACT

We present results of the measurement of the low frequency spectrum of solvated urea. The study revealed a blue shift of the intramolecular mode of urea centered at 150 cm^{-1} of $\Delta\nu = 17\ cm^{-1}$ upon increasing the pressure up to 10 kbar. The blue shift scaled linearly with the increase in density and was attributed to a stiffening of the water-urea intermolecular potential. We deduced an increase in the number of affected water molecules from 1 to 2 up to 5–7, which corresponds to the sterical coordination number of urea. The increase in hydration number can be explained by an suppression of the NH_2 inversion and the hydrogen bond switching around the NH_2 group. Pressure induced sterical constraints are proposed to hinder the rapid switching of hydrogen bond partners and make the water around urea less bulk-like than under ambient conditions.

1. Introduction

Pressures relevant for studies of biochemical systems generally range from 1 bar to 10 (1 bar = 0.1 MPa, 10 bar = 1 GPa). Although hydrostatic pressure significantly influences the structural properties and thus functional characteristics of cells, this has not prevented life from invading the cold and high pressure habitats of marine depths. 70% of the surface of the Earth is covered by oceans, and the average pressure on the ocean floor is about 400 bar. Psychrophilic-piezophilic (cold- and pressure-adapted) species, which live at ca. 2 °C, are found on the deepest ocean floor (ca. 11,000 m) in the Mariana Trench and in deep sea sediments, the so-called deep biosphere [1]. Close to hydrothermal vents, generally several thousand meters under the sea surface, even organisms far more complex than bacteria can be found at conditions of high hydrostatic pressure (HHP) (ca. 300 bar) and high temperature (up to ≈ 120 °C) [2,3].

* Corresponding author.
E-mail address: martina.havenith@rub.de (M. Havenith).

https://doi.org/10.1016/j.bpc.2019.106240
Received 3 June 2019; Received in revised form 14 July 2019; Accepted 27 July 2019
Available online 06 August 2019

Biological species which are subject to high hydrostatic pressure are known to have developed a variety of mechanisms in order to counteract the adverse effects of their environment towards cellular functioning: [4] Organic osmolytes such as amino acids, sugars, trimethylamine-N-oxide (TMAO) and urea have been found to be accumulated in life under extreme conditions regarding pressure and thermal stress [5].

It is a prerequisite for life under extreme conditions that denaturation of proteins by high pressure must be avoided. However, upon compression, a different state of the protein can become thermodynamically more favorable, thus initiating aggregation or unfolding. As a consequence, buried polar groups may become accessible which will change the hydration at the surface [6]. Previously, we could show that the dynamics of the hydrogen bond network in the hydration shell of proteins differs from bulk water or the buffer [7,8]. These changes in hydration dynamics are found to be correlated with protein function. In a ternary mixture, we have a more complex scenario which involves the interaction between protein, solvent and the cosolvent. The binding sites of the protein can either preferentially bind a cosolvent or preferentially exclude a cosolvent (preferential hydration) [9]. For osmolytes that stabilize the protein by direct interaction, such as urea, preferential binding to the protein backbone has been found to play a major role [10]. For TMAO, on the other hand, THz absorption studies suggest that an indirect, water-mediated effect might be responsible for its osmoprotective properties [11].

In deep sea animals living under high pressure, a mixture of TMAO and urea has been found to be enriched in cells, counteracting the denaturing effect of high pressure.

Typically, the amount of TMAO in cells and the ratio of concentrations (c_{TMAO}/c_{Urea}) was found to increase from 1 : 2 for fishes which live close to the surface up to 2 : 1 for fishes thriving around 2850 m below sea level [12–14].

On a molecular level, it is unclear whether and how these two osmolytes are counteracting the adverse effects of high hydrostatic pressure. High-pressure X-ray, FTIR and computational studies on TMAO showed, that upon addition of TMAO the *H*-bonds are strengthened and the second hydration shell is found to be moving slightly outward. This counteracts the effect of high hydrostatic pressure [15–19].

Interestingly, Meersman et al. observed for a urea-TMAO mixture of 1 : 2 a counteracting effect on the interaction potential, with TMAO and urea increasing and decreasing the attractive part of the protein-protein interaction, respectively [20]. No further increase in interaction was found for a 2 : 1 TMAO/urea solution above 2 kbar. It should be pointed out, that a 2 : 1 ratio of TMAO/urea is also typically detected in deep sea animals which have to withstand high hydrostatic pressure.

It could not yet be revealed whether the osmoprotective properties of ternary mixture are related to any cooperative effect. In an inelastic X-ray scattering study of osmolyte mixtures, Sahle et al. found a simple spectral additivity of the binary solution contributions, and deduced that the effect of direct interaction is small, if any [21]. In contrast to this, Hunger et al. determined a nonlinear increase in solute reorientation times in equimolar mixtures of TMAO and urea by means of dielectric spectroscopy, which suggests a cooperative effect [22]. By MD simulations, Smolin et al. could show that the presence of urea drives TMAO out of the hydration shell of SNase and interpreted this in terms of an osmophobic effect [23]. Studying RNase in naturally occuring osmolyte mixtures, Arns et al. revealed that TMAO is the predominant factor for the osmoprotective properties of these cosolvent mixtures. Glycine is suggested to stabilize proteins by direct interaction with the backbone or amino acid side chains rather than affecting the solvent-protein interaction [24]. Considering the denaturing properties of urea via direct interaction with the protein, MD simulations by Ganguly et al. on small peptides showed that TMAO inhibits the preferential interaction between proteins and urea [25]. This effect depends on the composition of the peptide. The presence of both urea and TMAO in osmolyte mixtures, which is found in fishes which survive under high pressure conditions might be required in order to compensate the perturbing effect on proteins of each of these osmolytes, as revealed by Hong et al.. According to their study, they propose that TMAO promotes aggregation of amyloidogenic intrinsically disordered peptides [26].

In general, solvent-mediated effects are expected to play a major role in protein stabilization under HHP conditions: Krywka et al. could demonstrate a reduction of temperature and pressure stability of SNase by urea using high-pressure SAXS measurements [27], which underlines the biological importance.

Under ambient conditions, urea serves as a well-known denaturant for proteins. Still, there has been a long standing controversial debate of whether urea can be regarded as structure breaker or a structure maker under these conditions. Similarly, the molecular mechanism which drives denaturation was controversially debated. Different mechanisms have been discussed in the literature: Initially, urea was proposed to be structure breaker of the water hydrogen bond network causing an increased solvation of hydrophobic groups [28]. This model was supported by NMR measurements [29], Raman spectra [30,31], molecular dynamics (MD) simulations [32] and by viscosity measurements of aqueous urea mixtures [33,34]. However, pump-probe IR-measurements [35], NMR [36], and neutron diffraction studies [37], as well as THz studies questioned the structure breaking hypothesis [38].

MD simulations by Hua et al.[39] showed that for hen lysozyme, urea unfolds the protein in a 2-stage process: In a first step, water is excluded from the protein solvation shell by direct binding of urea, causing a swelling of the lysozyme. In a second step, urea and water will solvate the protein interior. The preferential binding of urea to the hydrophobic parts of protein was suggested to lead to a dewetting and weakening of the hydrophobic effect [40,41]

In a MD study of solvated urea by Stumpe et al.[42] no indication of water structure breaking was found. Instead, the energy of the water-water HB was found to increase with increasing urea concentration. Idrissi et al. predicted a decrease of the tetrahedral arrangement of water [32]. However, more recently, Bandyopadhyay et al.[43] showed that the tetrahedral arrangement is conserved when taking into consideration the urea-urea interaction in dense solutions. This theoretical prediction is in agreement with the results of dielectric spectroscopy: Hayashi et al. [44] observed no significant preference for hydrogen bonding between urea with either urea or water.

Here, we use THz absorption spectroscopy to probe the hydration of urea under high pressure conditions. In our previous THz study of solvated urea under ambient conditions [38], we found that urea - in stark contrast to TMAO [11] - has a very weak impact on the water network and a small hydration shell with only $\approx 1-2$ water molecules bound to the urea on average. Using a semi-ideal chemical association model and accompanying MD simulations, the observed spectra could be decomposed into three contributions: One is attributed to bulk water, a second was initially assigned to a rattling mode of weakly solvated urea in the surrounding water cage and the third part accounts for THz modes describing a doubly hydrogen-bonded strong solute-solvent interaction. However, new measurements by Shiraga et al.[45] showed that the mode at ~ 4 THz or $\nu_0 \approx 150\ \mathrm{cm}^{-1}$ is not only present in an aqueous solution but is also observed in urea solutions with DMSO as a solvent. Thus, they reassigned this mode to a librational motion of a single urea molecule within the solvent cage [46]. Both THz studies yielded a small number of water molecules (1–2) which are affected per urea molecules: $n_{\mathrm{hydration}}$ was determined to be 1–2 independent of concentration. This implies that under ambient conditions the influence is restricted to one or two water at the acceptor H—B of oxygenation of urea only, which is significant less than the coordination number (4.1–6.3), i.e. the number of water in the first hydration shell.

This conclusion was supported based on an X-ray Raman scattering study of Sahle et al.[21] who suggested a minor impact of urea on the water structure. The small number of waters affected upon hydration of urea is also in line with compressibility data and broadband dielectric

studies [47].

In the following we will focus on the effect of high pressure on the hydration properties of urea. So far, only few experimental studies have been reported with controversial or ambiguous results [48]. Based on thermodynamic data, i.e. the derivative of the apparent molar volume of urea in the dilute limit and a negative shift of the point of maximum water density, Makarov et al. concluded that under high pressure conditions, urea acts as a structure breaking molecule [49].

2. Experimental results

We have measured the low frequency spectrum of 1.5 M solutions of urea in the pressure range up to 11 kbar using a diamond anvil cell and a FT spectrometer. The experiment has been described in detail in reference [46].

The transmitted intensity at the detector is given by:

$$I(p) = I_0 \exp\{-\alpha_p d_p\}/\exp\{-\alpha_0 d_0\}, \tag{1}$$

where I_p describes the transmitted intensity at given pressure p, I_0 the transmitted intensity at ambient pressure, $\alpha_p(\nu)$ the pressure dependent absorption, $\alpha_0(\nu)$ the absorption coefficient of the solvated urea at ambient conditions and d_p the sample thickness, which varies with pressure.

Here, we have to take into accout that the cell thickness can vary with increasing pressure, thus we obtain:

$$I(p) = I_0 \exp\{-\alpha_0 (d_p - d_0)\} \exp\{-\Delta\alpha d_p\}, \tag{2}$$

where α_0 corresponds to the absorption of the solution at ambient pressure, d_p and d_0 is the cell thickness at pressure p and at ambient conditions, respectively and $\Delta\alpha = \alpha_p - \alpha_0$.

We use

$$\alpha_p = -\ln\left\{\frac{I_p}{I_{ref}}\right\}\cdot\frac{1}{d_p} \tag{3}$$

$$\alpha_0 = -\ln\left\{\frac{I_0}{I_{ref}}\right\}\cdot\frac{1}{d_0} \tag{4}$$

and $\alpha_p = \alpha_0 + \Delta\alpha = \alpha_0 + (\alpha_p - \alpha_0)$, with I_{ref} corresponding to the transmission of the empty cell.

I_{ref} is a scaling factor for the recorded transmitted intensity, as can be seen in Eqs. (3) and (4). Since α_0 is well known from our previous measurements [38], we can adjust I_{ref} such that it reproduces the absorption of the solution under ambient conditions. For the pressurized sample the same value I_{ref} is used, since this will be unaffected by changes in the sample thickness. If we define our scale such that $I_{ref} = 1$, we obtain:

$$\alpha_p = \frac{\ln\{I_0\}}{d_0} - \frac{\ln\{I_p\}}{d_p} + \alpha_0. \tag{5}$$

Three data sets have been recorded separately using our high pressure THz set-up in Bochum. In addition to the data set in Bochum (up to 8 kbar, one high-resolution data set has been recorded at the synchrotron source SOLEIL, beam line AILES which provides data up to 12 kbar. The absorption spectra are shown in Fig. 1.

In order to determine spectral changes due to the presence of urea, first, the spectrum of pure water at the same pressure is subtracted.

$$\Delta\alpha = \alpha_p^{sol} - \alpha_p^{w} \tag{6}$$

with *sol* and *w* referring to the solution and water, respectively.

This would hold in case that changes in water concentration in the aqueous solution upon increasing pressure could be neglected. However, in order to correct for pressure induced changes, in a second step, we corrected for changes in density:

$$\alpha_{tot}[p] = x_s \cdot c[p] \cdot \varepsilon_s[p] + x_w \cdot c[p] \cdot \varepsilon_w[p] \tag{7}$$

where w and s refer to contributions of water and solute s, respectively. $c[p] = c_{sol}[p] + c_w[p]$ denotes the pressure-dependent total molar concentration in the solution. (Mole fractions x_s and x_w are used in order to reduce the number of pressure-dependent parameters.) The correction for the change in water concentration can now be described by

$$\frac{\Delta\alpha[p]}{c[p]} = x_s\varepsilon_s[p] - x_w\varepsilon_w[p](1-\beta) \tag{8}$$

and

$$\beta = \frac{\rho_{sol}[p] - M_S x_s c[p]}{\rho_w[p]} \tag{9}$$

with ρ_{sol}, ρ_w and M_S being the density of the solution. Based upon (8) and (9), we can deduce the following relation for the partial solute extinction:

$$\varepsilon_s[p] = \frac{1}{x_s}\left(\frac{\Delta\alpha[p]}{c[p]} + x_w\varepsilon_w\left(1 - \frac{\rho_{sol}[p] - M_S x_s c[p]}{\rho_w[p]}\right)\right) \tag{10}$$

However, in order to determine the partial solute extinction, the volumetric properties at high hydrostatic pressures, namely $c[p]$, $\rho_{sol}[p]$ and $\rho_w[p]$ must be known. Whereas for bulk water, ρ[p] data are available (see [50]), for most of the aqueous solutions c[p], ρ_{sol}[p] is not easy to determine experimentally. Thus, we fitted simultaneously a set of both experimental studies and results from theoretical modeling to deduce the pressure dependence of the density of urea solutions at high hydrostatic pressure [49,51–53]. For details, see the SI.

In Fig. 2, we show the partial solute extinction coefficient $\varepsilon_s(\tilde{\nu})$ at 1 bar, 4 kbar, 8 kbar and 10 kbar. An overview of all results is shown in the inset and in the SI.

At ambient conditions, the concentration and temperature dependent THz spectra of urea could be decomposed into three partial contributions: One is attributed to bulk water, a second one to rattling modes of weakly solvated urea in the surrounding water cage, and the third part accounts for THz modes describing a doubly hydrogen bonded strong solvent solute interaction. The latter one is increasing non-linearly with concentration and can be neglected for more dilute solutions. Even at 10 M (urea/water = 1 : 3) concentration, 80 of urea is not forming a strong urea water complex and the fraction of water in such complexes is on the order of a few percent [45].

In the present study of a urea solution with a concentration of 1.5 M, we restricted the decomposition of the THz spectra (after subtraction of bulk water) into a superposition of two damped harmonic oscillators, see: [11,54,55].

$$f(\nu, \nu_0, I_0, \Delta) = \frac{I_0 \nu^2 \Delta^2}{4\pi^3\left(\left(\nu_0^2 + \left(\frac{\Delta}{2\pi}\right)^2 - \nu^2\right)^2 + 4\left(\frac{\Delta}{2\pi}\right)^2\nu^2\right)}, \tag{11}$$

where I_0, Δ and ν_0 are the amplitude, the line-width and the reduced center frequency. For convenience, the wave number $\tilde{\nu}$ is used instead of the frequency ν.

Two additional terms are added to describe a) the low frequency part of the observed spectrum and b) the effect of volume exclusion of bulk water: When studying sugars in a THz difference spectrometer, it became evident, that a model of a simple three-component mixture fails to describe the change in absorption [56,57]. Next to bulk water, the solute itself and the lack of absorption due to volume exclusion by the solute or density change, an additional component was required. The latter was identified as hydration water, i.e. water within the solvation shell of a molecule that is characterized by an absorption which differs from those of bulk water. Thus, any change â€ “even after density correction- can be described by a positive contribution describing the spectral response of hydration water and a negative contribution, which describes the lack of water molecules which show a bulk-like spectral response. This latter is described as: $\varepsilon_w(p) \cdot n_h$, with $\varepsilon_w(p)$ and n_h, corresponding to the extinction coefficient of bulk water at a given

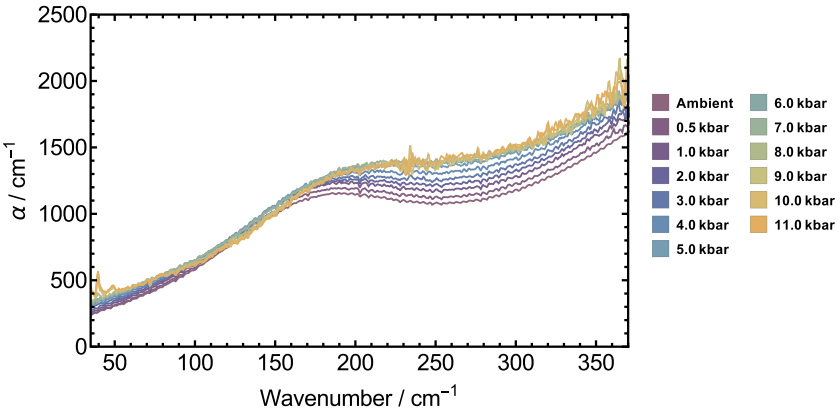

Fig. 1. Absorption coefficient $\alpha(\tilde{\nu})$ of aqueous (1.5 M) solution of urea at ambient $T \approx 296$K as a function of pressure.

pressure p, and the effective number of water molecules which are not bulk-like, respectively. n_h corresponds to the smallest number of water molecules which have an absorption distinct from bulk water, yielding a lower bound, i.e. the minimum, or effective number of hydration water molecules.

The dissected spectrum is displayed in Fig. 3 for $p =$ 1 bar, 4 kbar, 8 kbar and 10 kbar.

The mode at $\tilde{\nu} \approx 153\,\mathrm{cm}^{-1}$ (at $p =$ 1 bar) is assigned to the translational and rotational rattling mode of the weakly hydrated urea [38].

Up to 1 kbar, we observe an increase in the fitted amplitude of the partial component attributed to the urea rattling mode. The pressure-induced change of the peak frequency is plotted in Fig. 4. Up to 10 kbar we find a pressure-induced blue shift of ca. $17\,\mathrm{cm}^{-1}$ which is linearly correlated with the increase in density. We attribute the blue shift to a stiffening of the urea-water potential due to the increase in density, and hence a decrease in the average urea-water distance.

Under ambient pressure conditions, our THz study revealed a very small average number of affected water molecules: The effective number of water molecules in the hydration shell is ranging from 0.5 water molecules at 0 °C to 1.1 water molecules at 36 °C [38]. On average ≈1 to 2 water molecules are affected by urea and show a THz response distinct from bulk water. Based on the measurements reported here, we can deduce the effective number of hydration waters n_{hydr} as a function of pressure. Up to 8 kbar, n_{hydr} was found to increase from 0.7 to 4. For higher pressures (8 kbar – 12 kbar), this number is further increased to $5 \leq n_{\mathrm{hydr}} \leq 8$, see Fig. 5.

The observed increase in $n_{\mathrm{hydration}}$ is linearly correlated with the pressure induced increase of density. Thus, we also plot in the inset of Fig. 5, the number of hydration water $n_{\mathrm{hydration}}$ as a function of density.

The increase in $n_{\mathrm{hydration}}$ is in line with the results of Stumpe et al., who predicted an increase in the water-water-HB upon increasing urea concentration. Our results clearly reveal that more water are affected at high pressure than under ambient conditions. Thus urea is affecting more and more water molecules which are still "bulk-like" under ambient conditions.

In summary, we recorded the low frequency spectrum of solvated urea as a function of pressure up to 10 kbar. Our study reveals an increase in the hydration shell which is linearly correlated with an increase in density. The pressure induced blue shift of solvated urea is smaller than the pressure induced blue shift of the intermolecular stretch of the hydrogen-bond network of bulk water. This observation confirms the reassignment of the $140\,\mathrm{cm}^{-1}$ mode to the librational mode of urea in its hydration cage, which is not strongly coupled to the water network.

3. Conclusion

Here, we present results of a THz spectroscopic study of solvated urea under HPP conditions.

Our measurements reveal a blue shift of $17\,\mathrm{cm}^{-1}$ for the band centered at $150\,\mathrm{cm}^{-1}$ which is assigned to an intermolecular mode, i.e. a librational mode of urea in the H-bond network. We propose that the frequency shift is caused by a stiffening of urea-water network potential which causes a blue shift of the librational mode. This is supported by the fact that the blue shift is linearly correlated with an increase in density. Interestingly, the number of water molecules which are affected or retarded by urea increases from $n = 1$–2 at ambient condition to $5 \leq n \leq 7$ at pressures up to 10 kbar. We want to point out, that 6 water molecules correspond to the geometrical coordination number of urea. The HB lifetime of the non hydrogen bonded water is decreased in

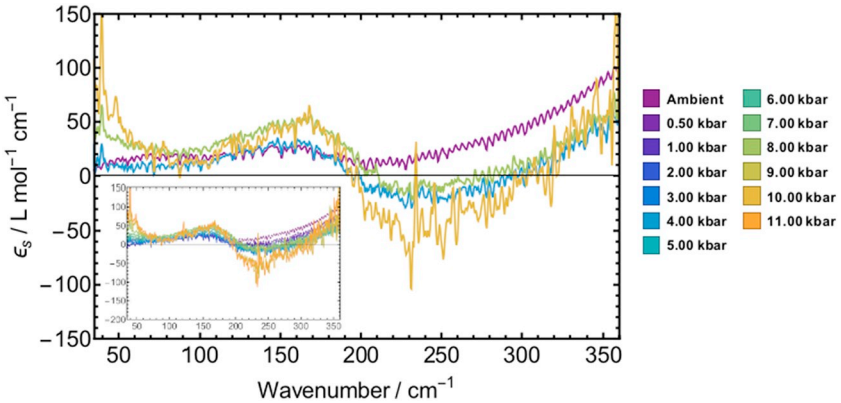

Fig. 2. Partial solute extinction coefficient $\varepsilon_s(\tilde{\nu})$ of urea at ambient conditions ($p =$ 1 bar, $T \approx$ 296 K) and at the pressures $p =$ 4 kbar, 8 kbar and 10 kbar. The full set of recorded spectra is shown in the inset.

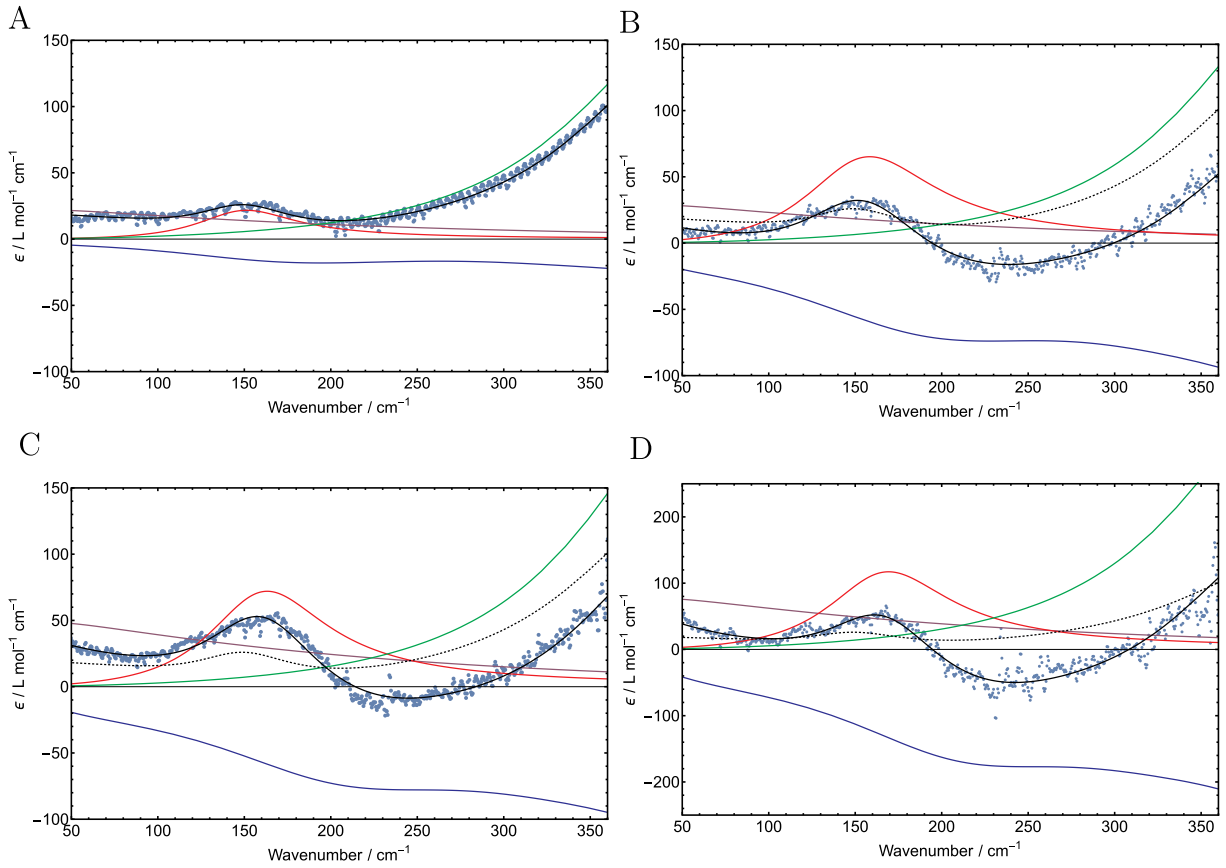

Fig. 3. Dissection of the partial solute extinction of urea at ambient pressure (A), 4 kbar (B), 8 kbar (C) and 10 kbar (D). The spectra were fitted using a low-frequency contribution [purple], a rattling mode of urea at $\tilde{\nu} \approx 153\,\mathrm{cm}^{-1}$ [red] and a barely resolved high frequency contribution [green]. The negative contribution describes the lack of bulk-like water - which is replaced by hydration water [blue]. The overall fit is shown in black. (For interpretation of the references to colour in this figure legend, the reader is referred to the web version of this article.)

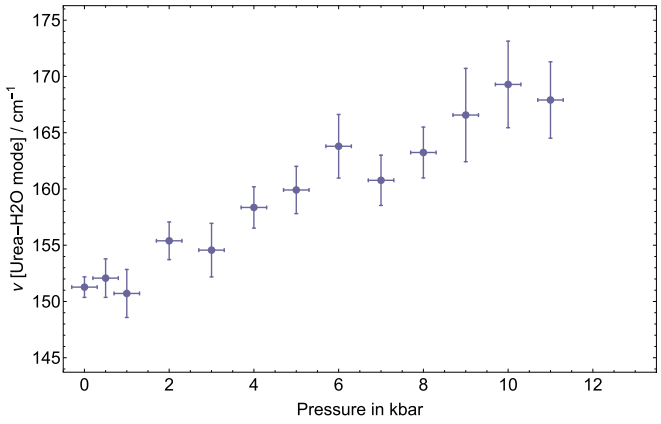

Fig. 4. Fitted center frequency ν_c of the intermolecular mode of urea.

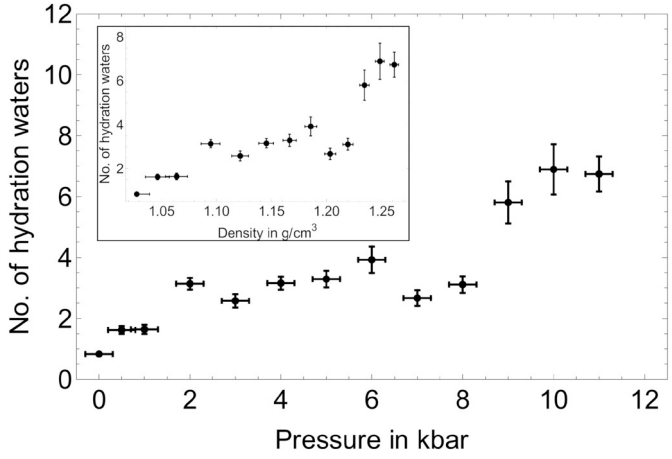

Fig. 5. Increase in $n_{\mathrm{hydration}}$ as function of pressure and inset: as function of density.

the vicinity of the NH_2 group compared to the in-plane water molecules at the acception in H-bond. It was argued that the NH_2 inversion motion which facilitates HB switching of HB partners and the formation of bulk-like HB in urea's out of plane direction, in contrast to the in-plane direction where the movement is restricted. In line with this model we propose now, that upon increasing the density, the large amplitude NH_2 inversion is more and more hindered. This pressure induced sterical constraint hinders the rapid switching of HB partners. We propose that as a result water around urea becomes less and less bulk-like upon increase of pressure. Thus, at 10 kbar not only the in-plane but also the out of plane water molecules are hindered. The effective number of water which are affected increases from 1 to 2 localized at the urea oxygen atom to 5–7, which corresponds to the geometrical coordination number.

4. Experimental

Samples of 1.5 M urea solution were prepared from urea (CAS 57–13-6) as purchased from Sigma (purum ≥99.0%, Sigma-Aldrich, München, Germany). The substance was weighed into ultra pure water from a water

treatment system (ASTM I, TKA Wasseraufbereitungssysteme, Niederelbert, Germany) using a precision scale (ABT 220–5 DM, Kern, Balingen, Germany). The concentration was verified by density measurements, using a vibrating tube density-meter (Anton Paar DMA 58, Anton Paar, Graz, Austria). Prior to using the sample for measurements, the aqueous solution was subject to a treatment of about 30 min in an ultrasonic bath in order to reduce the amount of dissolved gas.

Measurements at pressures up to 8 kbar were carried out using a commercial FTIR spectrometer (Bruker Vertex 80 V, Bruker, Ettlingen, Germany) with an external liquid He-cooled bolometer (Infrared Laboratories, Inc., Tucson, AZ, USA) as the detector and a mercury gas lamp as the source. Details concerning specific adaptations can be found elsewhere [46,58]. For these measurements, a commercially available Diamond Anvil Cell [DAC] (Almax Easylab VivoDAC, Almax Easylab, Diksmuide, Belgium), consisting of a diamond anvil and a flat diamond window, was used. Brass rings with an outer diameter of 3.95 mm, an inner diameter of 0.5 mm and a thickness of approximately 40μm, as manufactured by LMB Automation (Iserlohn, Germany), were used as gaskets without any preindentation. After filling the cell with the sample, the DAC was closed by applying a torque of 3.5 Nm using a torque wrench. The spectrometer was evacuated and spectra were recorded with a resolution of 1 cm^{-1}, averaging over 64 datasets. The absolute pressure inside the cell was determined with an accuracy of about 300 bar, employing a pressure-dependent shift of an absorption band in crystalline quartz, see Ref. 46. In order to avoid artifacts due to contributions of interfacial water at the quartz-water interface, we first determined the relation between internal sample pressure and external gas membrane pressure and used this relation to determine pressure. The changes in the thickness of the sample cell as a function of gas membrane pressure were measured ex-situ using two confocal distance sensors (Micro-Epsilon IFS 2403, Micro-Epsilon, Ortenburg, Germany). We could reach pressures up to 8 kbar. Details are described in[58] and the corresponding supplementary information.

Additional measurements have also been performed at the beamline AILES [59] at SOLEIL. In these measurements, higher intensities and higher pressures (up to 11 kbar) could be achieved. For the high pressure setup at AILES a commercial FTIR spectrometer has been adapted. The full setup has been described elsewhere [60]. For these measurements a diamond anvil cell from BETSA (Nangis, France), consisting of two diamond anvils, was used. Thinner gaskets with a thickness of approximately 30 µm, manufactured by LMB Automation (Iserlohn, Germany), could be used as well in order to obtain a higher intensity at the detector. Using the fluorescence of small Ruby spheres that could be excited in-situ the pressure in the cell was determined [60,61] with an accuracy of about 0.4 kbar, only restrained by the calibration curve in the relevant regime [62]. For these measurements, the thickness was determined by minimizing the distance-squared between spectra recorded in Bochum and measurements performed at AILES and by linear extrapolation towards higher pressures. In both setups, the DAC was pressurized by means of a gas membrane using an automated pressurizing system (Pace 5000, GE Measurement, Billerica, MA, USA) In order to achieve pressure equilibration, spectra were recorded 3 minutes after the pressure was adjusted.

All calculations have been performed using Mathematica 10. (Wolfram Research, Champaign, IL, USA).

Acknowledgement

The authors thank M.Sc. Katja Mauelshagen for assistance in the lab and the beamline staff at AILES at SOLEIL. This work is supported by the Forschergruppe (FOR 1979 - “ Exploring the Dynamical Landscape of Biomolecular Systems by Pressure Perturbation”) and part of the Cluster of Excellence RESOLV (EXC 2033), funded by the Deutsche Forschungsgemeinschaft (Germany). Measurements have been performed at AILES, SOLEIL (Proposal no. 20160970). We acknowledge SOLEIL for provision of synchrotron radiation facilities and we would like to thank Francesco Capitani for assistance.

Appendix A. Supplementary data

Supplementary data to this article can be found online at https://doi.org/10.1016/j.bpc.2019.106240.

References

[1] P.M. Oger, M. Jebbar, Res. Microbiol. 161 (2010) 799–809.
[2] A.A. Yayanos, Proc. Natl. Acad. Sci. U. S. A. 83 (1986) 9542–9546.
[3] F.M. Lauro, D.H. Bartlett, Extremophiles 12 (2008) 15–25.
[4] P.H. Yancey, M.E. Clark, S.C. Hand, R.D. Bowlus, G.N. Somero, Science 217 (1982) 1214–1222.
[5] P.H. Yancey, J. Exp. Biol. 208 (2005) 2819–2830.
[6] C. Braz Royer, J. Med. Biol. Res. 38 (2005) 1167–1173.
[7] M. Grossman, B. Born, M. Heyden, D. Tworowski, G.B. Fields, I. Sagi, M. Havenith, Nat. Struct. Mol. Biol. 18 (2011) 1102–1109.
[8] M. Heyden, D.J. Tobias, Phys. Rev. Lett. 111 (2013) 218101.
[9] S.N. Timasheff, Proc. Natl. Acad. Sci. U. S. A. 99 (2002) 9721–9726.
[10] Y. Liu, B.D. W, Biochemistry 34 (1995) 12884–12891.
[11] L. Knake, K. Kartaschew, G. Schwaab, M. Havenith, J. Phys. Chem. B 119 (2015) 13842–13851.
[12] R.H. Kelly, P.H. Yancey, Biol. Bull. 196 (1999) 18–25.
[13] J.R. Treberg, W.R. Driedzic, J. Exp. Zool. 293 (2002) 39–45.
[14] C.J. Laxson, N.E. Condon, J.C. Drazen, P.H. Yancey, Physiol. Biochem. Zool. 84 (2011) 494–505.
[15] A. Panuszko, P. Bruzdziak, J. Zielkiewicz, D. Wyrzykowski, J. Stangret, J. Phys. Chem. B 113 (2009) 14797–14809.
[16] B.J. Bennion, V. Daggett, Proc. Natl. Acad. Sci. U. S. A. 101 (2004) 6433–6438.
[17] H. Wei, Y. Fan, Y.Q. Gao, J. Phys. Chem. B 114 (2010) 557–568.
[18] A. Kuffel, J.J. Zielkiewicz, Chem. Phys. (2010) 133.
[19] M.A. Schroer, Y. Zhai, D.C.F. Wieland, C.J. Sahle, J. Nase, M. Paulus, M. Tolan, R. Winter, Angew. Chem. Int. Ed. 50 (2011) 11413–11416.
[20] F. Meersman, D. Bowron, A.K. Soper, M.H. Koch, J. Biophys J 97 (2009) 2559–2566.
[21] C.J. Sahle, M.A. Schroer, I. Juurinen, J. Niskanen, Phys. Chem. Chem. Phys. 18 (2016) 16518–16526.
[22] J. Hunger, N. Ottosson, K. Mazur, M. Bonn, H.J. Bakker, Phys. Chem. Chem. Phys. 17 (2015) 298–306.
[23] N. Smolin, V.P. Voloshin, A.V. Anikeenko, A. Geiger, R. Winter, N.N. Medvedev, Phys. Chem. Chem. Phys. 19 (2017) 6345–6357.
[24] L. Arns, V. Schuabb, S. Meichsner, M. Berghaus, R. Winter, Z. Phys. Chem. 232 (2018) 615–634.
[25] P. Ganguly, P. Boserman, N.F.A. Van Der Vegt, J.E. Shea, J. Am. Chem. Soc. 140 (2018) 483–492.
[26] S. Hong, Jiang Xiong, Biophys. J. 111 (2016) 1866–1875.
[27] C. Krywka, C. Sternemann, M. Paulus, M. Tolan, C. Royer, R. Winter, ChemPhysChem 9 (2008) 2809–2815.
[28] H.S. Frank, F. Franks, J. Chem. Phys. 48 (1968) 4746–4757.
[29] E.G. Finer, F. Franks, M.J. Tait, J. Am. Chem. Soc. 94 (1972) 4424–4429.
[30] G.E. Walrafen, J. Chem. Phys. 44 (1966) 3726–3727.
[31] A. Idrissi, Spectrochim. Acta A 61 (2005) 1–17.
[32] M. Idrissi, P. Damay, M. Kiselev, Y. Puhovsky, E. Cinar, P. Lagant, G. Vergoten, G. A, J. Phys. Chem. B 114 (2010) 4731–4738.
[33] J.A. Rupley, J. Phys. Chem. 68 (1964) 2002–2003.
[34] T.T. Herskovits, T.M. Kelly, J. Phys. Chem. 77 (1973) 381–388.
[35] Y.L.A. Rezus, H.J. Bakker, Proc. Natl. Acad. Sci. U. S. A. 103 (2006) 18417–18420.
[36] A. Shimizu, K. Fumino, K. Yukiyasu, Y. Taniguchi, J. Mol. Liq. 85 (2000) 269–278.
[37] J. Turner, J.L. Finney, A.K. Soper, Z. Naturforsch. 46 (1991) 73–78.
[38] S. Funkner, M. Havenith, G. Schwaab, J. Phys. Chem. B 116 (2012) 13374–13380.
[39] L. Hua, R. Zhou, D. Thirumalai, B.J. Berne, Proc. Natl. Acad. Sci. U. S. A. 105 (2008) 16928–16933.
[40] S.J. Whittington, B.W. Chellgren, V.M. Hermann, T.P. Creamer, Biochemistry 44 (2005) 6269–6275.
[41] A.K. Soper, E.W. Castner, A. Luzar, Biophys. Chem. 105 (2003) 649–666.
[42] M.C. Stumpe, H. Grubmüller, J. Phys. Chem. B 111 (2007) 6220–6228.
[43] D. Bandyopadhyay, S. Mohan, S.K. Ghosh, N. Choudhury, J. Phys. Chem. B 118 (2014) 11757–11768.
[44] Y. Hayashi, Y. Katsumoto, S. Omori, N. Kishii, A. Yasuda, J. Phys. Chem. B 111 (2007) 1076–1080.
[45] K. Shiraga, Y. Ogawa, K. Tanaka, T. Arikawa, N. Yoshikawa, M. Nakamura, K. Ajito, T. Tajima, J. Phys. Chem. B 122 (2018) 1268–1277.
[46] L. Knake, H. Vondracek, M. Havenith, Rev. Sci. Instrum. 87 (2016) 1–5.
[47] U. Kaatze, J. Chem. Phys. 147 (2017) 024502.
[48] K. Yoshida, K. Ibuki, M. Ueno, J. Chem. Phys. 108 (1998) 1360–1367.
[49] D.M. Makarov, G.I. Egorov, J. Chem. Thermodyn. 120 (2018) 164–173.
[50] W. Wagner, A. Pruß, J. Phys. Chem. Ref. Data 31 (2002) 387–535.
[51] P. Salmen, Röntgenreflektometrie an der hydrophoben Festkörper-Flüssigkeits-Grenzfläche, Ph.D. thesis Technische Universität, Dortmund, Germany, 2017.
[52] C. Held, G. Sadowski, Fluid Phase Equilib. 407 (2016) 224–235.
[53] M. Knierbein, Personal Communication, 2017 (April 2017).
[54] V. Sharma, F. Böhm, M. Seitz, G. Schwaab, M. Havenith, Phys. Chem. Chem. Phys.

15 (2013) 8383.
[55] V. Sharma, F. Böhm, G. Schwaab, M. Havenith, Phys. Chem. Chem. Phys. 16 (2014) 25101–25110.
[56] U. Heugen, G. Schwaab, E. Bründermann, M. Heyden, X. Yu, D.M. Leitner, M. Havenith, Proc. Natl. Acad. Sci. U. S. A. 103 (2006) 12301–12306.
[57] M. Heyden, E. Bründermann, U. Heugen, G. Niehues, D.M. Leitner, M. Havenith, J. Am. Chem. Soc. 130 (2008) 5773–5779.
[58] H. Vondracek, S. Imoto, L. Knake, G. Schwaab, D. Marx, M. Havenith, In Preparation, (2018).
[59] P. Roy, M. Rouzières, Z. Qi, O. Chubar, Infrared Phys. Technol. 49 (2006) 139–146.
[60] A. Voute, M. Deutsch, A. Kalinko, F. Alabarse, J.-B. Brubach, F. Capitani, M. Chapuis, V. Ta Phuoc, R. Sopracase, P. Roy, Vib. Spectrosc. 86 (2016) 17–23.
[61] F. Datchi, A. Dewaele, P. Loubeyre, R. Letoullec, Y. Le Godec, B. Canny, High Pressure Res. 27 (2007) 447–463.
[62] W.L. Vos, J.A. Schouten, J. Appl. Phys. 69 (1991) 6744–6746.